minerals

MDPI

Article

Synthesis of Ye'elimite from Anthropogenic Waste

Robert Kusiorowski *, Barbara Lipowska and Anna Gerle

Łukasiewicz Research Network—Institute of Ceramics and Building Materials, Refractory Materials Centre in Gliwice, Toszecka 99, 44-100 Gliwice, Poland

* Correspondence: robert.kusiorowski@icimb.lukasiewicz.gov.pl

Abstract: Calcium sulphoaluminate cement (CSA) is characterized by a different chemical and mineralogical composition than common cements based mainly on Portland clinker. Its main component is ye'elimite—$Ca_4(AlO_2)_6SO_4$. This cement is characterized by a shorter setting time and a dynamic increase in strength in the early aging process. Currently, CSA cements are gaining more and more popularity due to their favorable ecological aspects, including a reduction in carbon dioxide emissions and negative impacts on the environment. The aim of the study was to determine the possibility of obtaining ye'elimite from waste materials of anthropogenic origin, which in this case were by-products from the aluminum anodizing process and cement–asbestos waste. The results of this preliminary research indicated the possibility of obtaining ye'elimite from secondary raw materials of anthropogenic origin. In each material, the phase of ye'elimite was identified to be the main mineral component, and the obtained materials displayed binding properties after mixing with water.

Keywords: cement–asbestos waste; anodizing aluminium sludge; ye'elimite; synthesis

Citation: Kusiorowski, R.; Lipowska, B.; Gerle, A. Synthesis of Ye'elimite from Anthropogenic Waste. *Minerals* **2023**, *13*, 137. https://doi.org/10.3390/min13020137

Academic Editor: Elsabe Kearsley

Received: 30 November 2022
Revised: 11 January 2023
Accepted: 14 January 2023
Published: 17 January 2023

1. Introduction

Calcium sulphoaluminate cement (CSA) is a low-energy cement that is produced at a lower temperature range than ordinary Portland cement. This cement is a relatively new and uncommon type of cement, invented by A. Klein in the 1950s [1]. Currently, it is widely used, mainly in China [2]. CSA clinker is a hydraulic binder obtained in the process of thermal treatment of limestone, bauxite, and gypsum at a temperature range between 1200 and 1300 °C [3].

The main component of CSA cement is ye'elimite; its formula is $Ca_4(AlO_2)_6SO_4$ ($C_4A_3\hat{S}$ in cement notation). In addition to this phase, CSA clinker and cement consists mainly of belite (C_2S) and calcium sulfate ($C\hat{S}$) or aluminoferrite (C_4AF) [4] in different proportions, depending on the application.

CSA cement is characterized by a quick onset of setting and a very rapid increase in early strength [5]. Moreover, products based on CSA cement are characterized by limited shrinkage or even slight expansion. This is due to the bonding process of the cement. In contrast to Portland cement, instead of so-called CSH phases and portlandite, the main product of CSA clinker hydration is ettringite ($C_6A\hat{S}_3H_{32}$) [1]. The formation of ettringite is responsible for the rapid increase in early strength and shrinkage reduction.

In addition, the formation of a large amount of ettringite is associated with the phenomenon of "self-drying" because, in the process of binding, a significant amount of water is needed to produce $C_6A\hat{S}_3H_{32}$ [5].

An important argument for the use of CSA cement is the ecological aspect. The emissions of carbon dioxide during the production of this type of cement are much lower. According to the literature [3,6], the reduction of CO_2 emissions in typical CSA cement production is approximately 1/3 compared to that of ordinary Portland cement. This is mainly due to three reasons: (a) reduction in the burning temperature by approximately 100–150 °C, (b) reduction in energy consumption during the grinding process due to easier

grindability, (c) reduction of CO_2 emissions due to a lower fraction of $CaCO_3$ in the raw materials [3].

Recently, increasing attention has been paid to issues related to sustainable development and the economy [7,8]. The transition to a sustainable economy will not be possible without the implementation of circular economy principles, including the reuse of raw materials and products or extending their lifespan, which in the long term is expected to bring benefits to the economy and the environment. One of the possible aims of implementing this policy is also to manage waste related to industrial–human activity.

In accordance with the waste management hierarchy, pursuant to the Waste Act [9,10], landfilling should be the ultimate solution, and if appropriate possibilities arise, other, less environmentally harmful methods of waste management should be applied. Such solutions should also be sought for various types of anthropogenic waste. The use of waste and by-products in construction is becoming common practice in many European countries and elsewhere [11]. Among many others, the following two types of waste related to industrial–human activity should be considered.

The first is cement–asbestos waste. Prompted by the recent European directives and resolutions [12], the need for safe disposal and/or internment of asbestos-containing materials should become a priority. The problem connected with asbestos waste is serious. According to estimates, there are approximately 15 million tons of asbestos-containing materials in Poland alone [13]. Most of them are in the form of cement–asbestos, which was widely used in the construction industry in the past [14]. However, the problem of asbestos is global [15–17]. Despite numerous restrictions on the use of asbestos, there are countries that continue to exploit, extract, and manufacture asbestos [18]. Although most of the extraction and manufacture of asbestos products in the world occurred in the past, the estimated worldwide consumption of asbestos fiber is still around 1.2 million tons per year [19].

In practice, the asbestos problem has not been solved on an industrial scale, and the neutralization of this waste on a mass scale currently involves landfilling. Researchers around the world are working on alternative methods of utilizing materials that contain asbestos fibers [20–22], but practically none of these methods have been applied on a large scale. This results from the fact that every treatment action of asbestos-containing material (including extraction, transport, application, fragmentation, and waste treatment) releases asbestos dust and fibers into the surrounding environment [23,24].

The second type of anthropogenic waste is by-products such as sludge from the process of aluminum anodizing. This sludge is a product of the neutralization of wastewater generated during the subsequent stages of aluminum anodizing. It consists mainly of colloidal aluminum hydroxide, sodium, or calcium hydroxides—depending on the type of neutralizing agent, aluminum sulfate and water [25]. The amounts of sludge produced in the aluminum anodizing process are significant. In the EU countries, it reaches approximately 100,000 tons per year [26]. Currently, similarly to asbestos wastes, it is mainly landfilled, which entails ever-increasing costs of transport and storage. It also poses a large environmental problem.

The aim of the presented study was to determine the possibility of synthesizing and obtaining ye'elimite from waste materials of anthropogenic origin. For this purpose, by-products from the aluminum anodizing process and cement–asbestos waste were used. This work can provide useful information about their safe recycling. With the development of safe technology, in the future, it will be rational and necessary to recycle this waste.

2. Materials and Methods

Two main kinds of anthropogenic waste were used in the study. First, cement–asbestos waste board was used as a representative of asbestos-containing material (ACM). It was selected due to the fact that it now represents the biggest group of ACM accumulated in the territory of Poland. To avoid the problem of secondary contamination of the environment by asbestos fibers, this waste was previously calcined (1200 °C/8 h) in a laboratory electric

furnace. After thermal treatment, the material was ground to achieve a fine powder (material AC). In the thermal treatment process, asbestos minerals transform into new mineral phases as a result of thermochemical reactions [27–30]. The second anthropogenic waste was wastewater neutralization sludge produced in the aluminum anodizing process (i.e., aluminum-anodizing sludge) provided by a domestic manufacturer of aluminum systems for the construction industry (material AL). Apart from the above-mentioned waste materials, chemical reagents and mineral resources were also used to correct the composition of the mix subjected to research. The components used were commercially available and had technical grades of purity. They included calcium carbonate (pure, Chempur, Piekary Śląskie, Poland), aluminum hydroxide (pure, Chempur, Piekary Śląskie, Poland), calcium sulfate hemihydrate (pure, Chempur, Piekary Śląskie, Poland), as well as limestone flour (technical grade, Lhoist, Tarnów Opolski, Poland), and bauxite flour (SG Mineral, Białystok, Poland). All the materials were subjected to chemical analysis (XRF), and their phase compositions were determined (XRD).

Seven research mixes (Table 1) were prepared based on these components. The goal was to obtain a chemical composition as close as possible to the stoichiometric proportion of individual oxides contained in ye'elimite $Ca_4(AlO_2)_6SO_4$. ACM waste was used as a source of calcium oxide and sulfur oxide, while aluminum-anodizing sludge was used as a source of aluminum oxide. All the components, carefully weighted to the predetermined proportion, were first homogenized in a corundum ball mill for 20 min and, next, formed as cylinders (~50 g of material, 35 mm in diameter, uniaxial pressing at 80 MPa). Then, the formed samples were fired in a laboratory electric furnace. This process was conducted at 1250, 1300, and 1350 °C for 4 h and at 1350 °C for 8 h, respectively. The temperature was selected based on the FactSage 6.4 calculation, which enabled a preliminary sinterability assessment. Finally, the samples were crushed and milled to powder fraction for XRD measurement. Based on the XRD results, four selected research mixes were prepared and fired (1350 °C/8 h) to obtain a larger amount of materials in order to determine the binding properties. After crushing in a single-toggle jaw crusher (Makrum, L44.41), the main properties of the obtained binders were tested according to the laboratory procedures. The following properties were determined: water–cement (w/c) ratio by standard consistency, bulk density, specific surface by the Blain method, initial and final setting time by the Vicat method, and compressive and flexural strength after 14 days of setting.

Table 1. List of tested materials.

Research Mix	Composition
A	$CaCO_3$ + $CaSO_4 \cdot 1/2H_2O$ + $Al(OH)_3$
B	limestone flour + bauxite flour + $CaSO_4 \cdot 1/2H_2O$
C	limestone flour + bauxite flour + AL material + $CaSO_4 \cdot 1/2H_2O$
C2	AL material + $Al(OH)_3$
D	bauxite flour + AC material + $CaSO_4 \cdot 1/2H_2O$
E	AC material + AL material + bauxite flour + $Al(OH)_3$ + $CaSO_4 \cdot 1/2H_2O$
F	AC material + AL material

The chemical analysis of the raw materials was performed by X-ray fluorescence (XRF; PANalytical, Almelo, The Netherlands), using a Panalytical Magix PW-2424 spectrometer, following the procedures contained in the PN-EN ISO 12677:2011 standard [31]. The chemical analysis was extended to include the content of volatile components, measured by calcination at 1025 °C and expressed as a value of loss on ignition (LOI). The phase compositions of the anthropogenic waste and the obtained products of synthesis were determined using powder X-ray diffraction (XRD; PANalytical, Almelo, The Netherlands). The analyses were conducted using a PANalytical X'pert Pro diffractometer (CuKα radiation, Ni filter, 40 kV, 30 mA, X'Celerator detector). The mineralogical quantitative phase analysis was performed using the Rietveld method. The microstructure of the samples was observed with a scanning electron microscope (Mira III; Tescan, Brno, Czech Repub-

lic) in combination with the Energy Dispersive Spectroscopy (EDS) system with AZtec Automated software (Oxford Instruments, Abingdon, UK).

3. Results and Discussion

3.1. Materials

As mentioned above, chemical reagents, natural raw materials, and two kinds of anthropogenic waste were used in the production of binders investigated in this study with regard to the synthesis of ye'elimite. The physical and chemical properties of the materials used are represented in Table 2.

Table 2. Chemical properties of the tested materials.

Component	Calcium Carbonate	Aluminium Hydroxide	Calcium Sulphate Hemihydrate	Limestone Flour	Bauxite Flour	AL Material	AC Material
CaO, %	56.03 ± 2.61	0.01 ± 0.01	43.17 ± 2.02	61.06 ± 2.85	0.20 ± 0.12	27.22 ± 1.28	59.81 ± 2.79
Al_2O_3, %	0.24 ± 0.12	61.33 ± 2.36	0.08 ± 0.08	0.31 ± 0.24	86.81 ± 3.33	21.45 ± 0.86	4.94 ± 0.31
SiO_2, %	0.14 ± 0.14	0.01 ± 0.01	0.52 ± 0.24	0.69 ± 0.31	6.38 ± 0.35	1.22 ± 0.32	23.81 ± 1.09
MnO, %	-	-	0.01 ± 0.03	0.01 ± 0.03	0.02 ± 0.03	0.01 ± 0.03	0.09 ± 0.03
Fe_2O_3, %	0.05 ± 0.07	0.01 ± 0.07	0.03 ± 0.07	0.31 ± 0.07	1.62 ± 0.07	0.19 ± 0.07	3.71 ± 0.11
MgO, %	0.13 ± 0.13	-	0.33 ± 0.31	0.27 ± 0.27	0.13 ± 0.13	0.56 ± 0.31	4.12 ± 0.37
Na_2O, %	0.01 ± 0.01	0.18 ± 0.14	0.01 ± 0.01	0.01 ± 0.01	0.02 ± 0.02	0.68 ± 0.15	0.05 ± 0.05
K_2O, %	-	-	0.01 ± 0.01	0.01 ± 0.01	0.22 ± 0.06	0.02 ± 0.02	0.05 ± 0.05
SO_3, %	-	-	57.18 ± 2.88	-	-	9.64 ± 0.82	1.66 ± 0.32
Loss on ignition, %	43.54 ± 6.53	37.91 ± 5.69	4.61 ± 0.69	37.47 ± 5.62	0.17 ± 0.03	37.36 ± 5.60	1.24 ± 0.19

The characteristics of chemical and mineral raw materials did not significantly depart from the expectations. As regards chemical raw materials, their high chemical purity was confirmed, and in the case of flours, it was confirmed that the main components were, respectively, calcium oxide (content of 97% after taking into account the loss on ignition in the case of lime powder, in the form of calcium carbonates and portlandite), and, in the case of bauxite flour, alumina (content at the level of 86%, in the form of phase corundum). In this section, special attention has been paid to the anthropogenic waste used. The first one was sludge from the aluminum anodizing process (AL waste), and the second was a raw as well as a thermally treated asbestos–cement product (AC waste).

In the case of AL waste, the main chemical components—after deducting the loss on ignition—were alumina and calcium oxide, in the amount of 35%–40% each, and a significant amount of sulfur compounds (Table 2). Regarding the phase, the material was dominated by the amorphous part, which was accompanied by calcite, gibbsite, ettringite, gypsum, and bassanite (Figure 1). Microstructure studies confirmed the fine-crystalline form of the waste, which tends to agglomerate the finest grains and form conglomerates (Figure 2).

In the case of raw AC waste, the main chemical components in the material were calcium and silicon oxides (Table 2). Mineral phases typical of the bound cement slurry were identified, e.g., portlandite, calcite, dicalcium silicate, ettringite, and katoite (Figure 3). The presence of a clearly increased background in the range of average angular values indicates a significant content of matter that does not have an ordered crystal structure. The identified phase composition of AC asbestos–cement waste is similar and close to that described in the literature [32–34]. SEM observations (Figure 4a), revealing typical fibrous forms, also confirmed the presence of asbestos minerals in the material: chrysotile and crocidolite—a fibrous form of riebeckite.

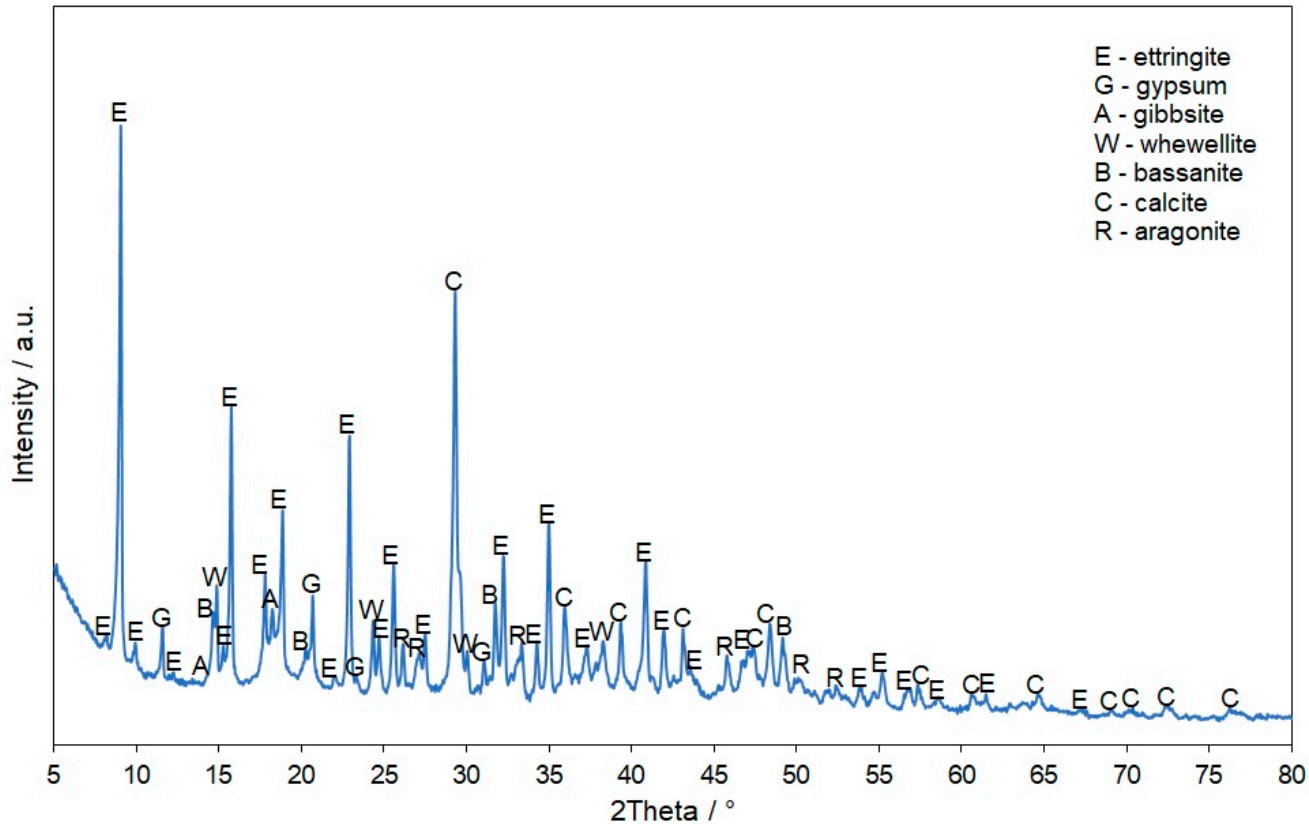

Figure 1. XRD pattern of AL sample.

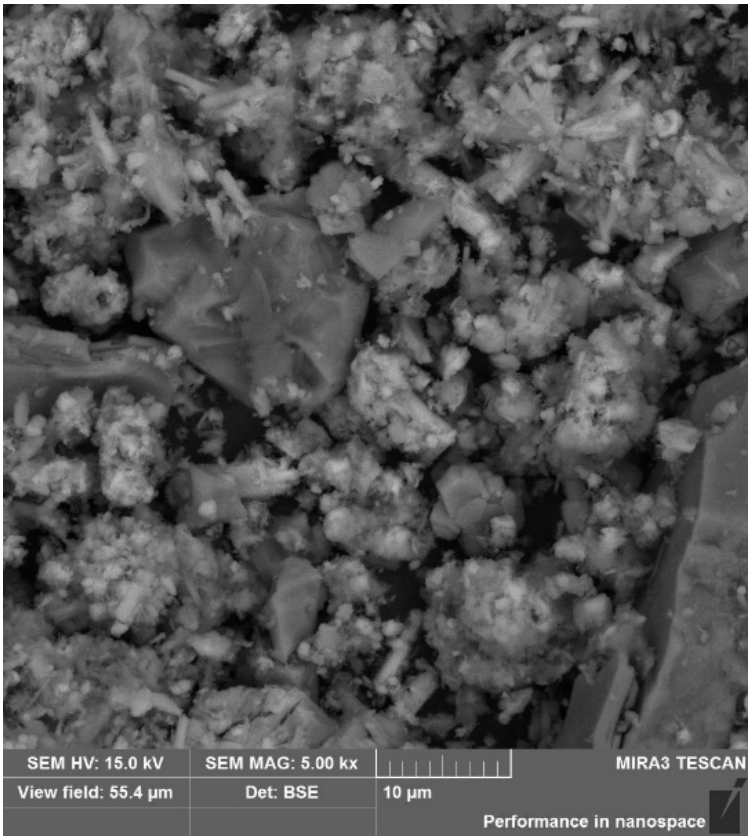

Figure 2. SEM image of AL sample.

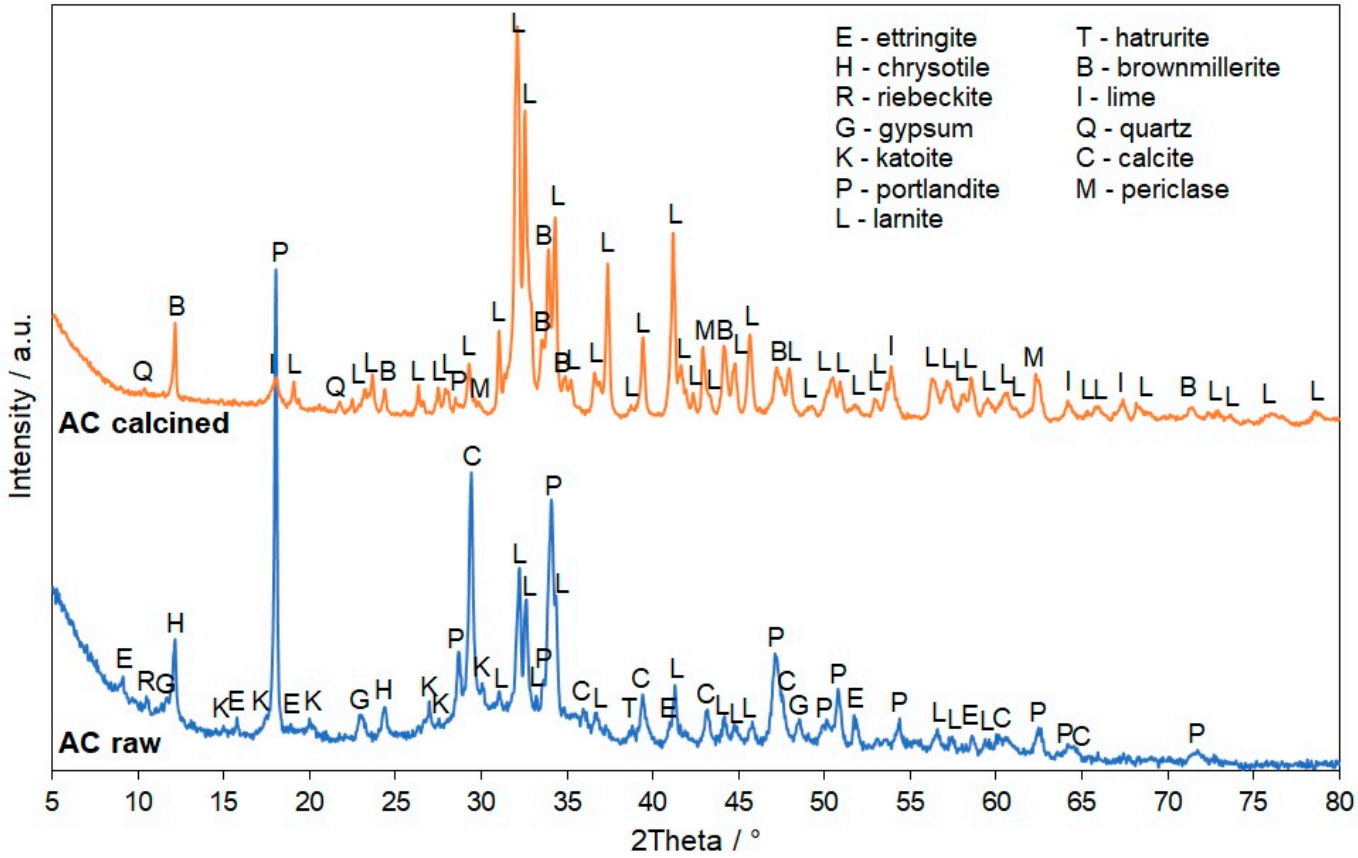

Figure 3. XRD patterns of AC sample, raw and after calcination.

In order to minimize the problem of contamination of the environment by asbestos fibers, AC waste was subjected to prior thermal treatment and, in the so-obtained form, was used in further stages of the research. During thermal treatment, cement–asbestos materials undergo a series of solid-state reactions leading to changes in the cementitious matrix and the crystal–chemical transformation of asbestos minerals [34,35]. Asbestos minerals were not identified in the material obtained as a result of AC waste pre-roasting (1200 °C/8 h), and the main components were dicalcium silicate—larnite, as well as lime, brownmillerite (Figure 3). This material was characterized by a high tendency to crumble (Figure 4b). SEM observations revealed a small presence of the so-called fiber pseudomorphs, having a clearly different crystalline structure, with grains of insular silicates, which enable easy crushing and grinding (Figure 4c). At a high magnification of fiber pseudomorphs, the pervasive recrystallization in micrometric grains is evident. This microstructure suggests that the original cleavage of the fibers along the fiber length is superseded by a parting along grain boundaries in the samples subjected to treatment, excluding the formation of hazardous fibrils [30,36].

3.2. Preliminary Synthesis

Based on the knowledge of the chemical composition of the selected raw materials and waste (Table 2), seven compositions of the test mixtures (Table 1) were composed so that the maximum possible amount of the desired component, i.e., ye'elimite, could be produced in terms of stoichiometry. For each set, based on the knowledge of the resultant chemical composition, the sinterability of the masses was determined by determining the amount of the liquid phase formed using FactSage 6.4 engineering software (Figure 5).

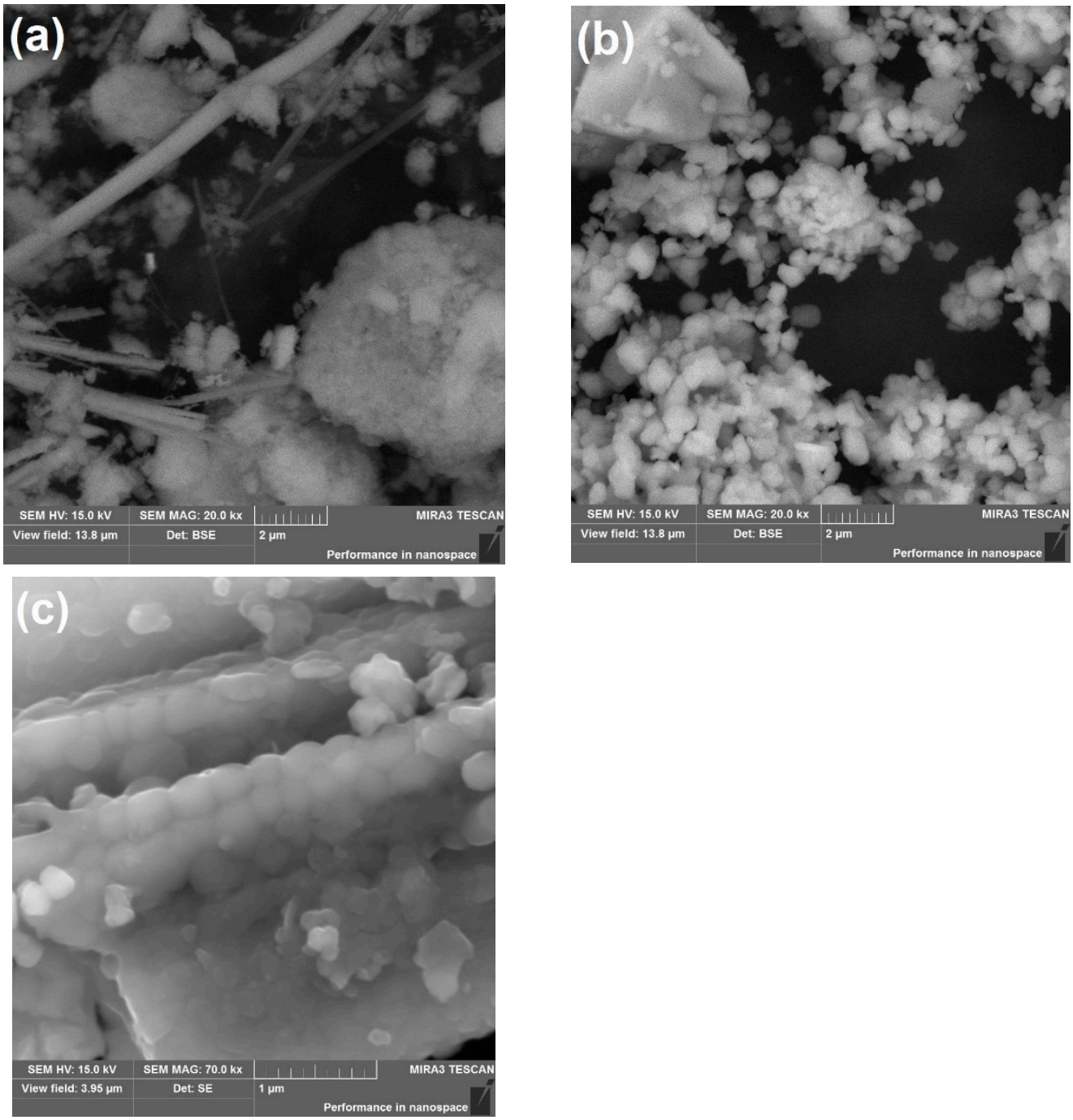

Figure 4. SEM image of AC sample: (**a**) raw, (**b**) calcined, (**c**) fiber pseudomorphs after calcination.

The conducted calculations indicate that at a relatively low firing temperature, the liquid phase will be formed in sets C2 and A. In the case of D, E, and F, the liquid phase will appear during firing and sintering at a temperature of 1150–1300 °C, with its highest amount recorded for set F. In the case of masses B and C, the liquid phase will appear the latest, according to the simulation, at a temperature of more than 1400 °C.

After firing in the assumed conditions, materials differing in the degree of sintering, expressed as the diameter of the fired materials, were obtained (Figure 6). Material shrinkage was evident in the case of sets C2 and F, whereas materials B, C, and D had significantly larger sizes than the formed samples. This effect can be directly related to the appearance of a liquid phase in the system during firing. In the case of materials for which calculations

in the FactSage program revealed the appearance of a liquid phase at a relatively lower temperature, a clear reduction in the dimensions of the fired moldings was observed.

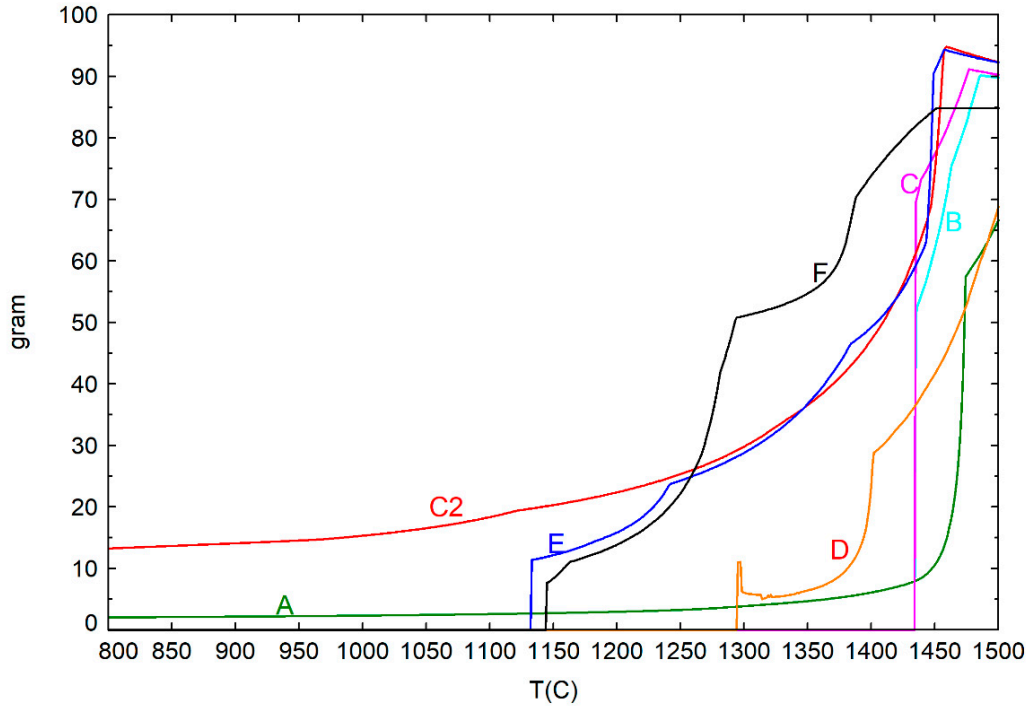

Figure 5. Simulation of liquid phase amount in considered research mixes.

Figure 6. Appearance of the materials obtained after synthesis at 1350 °C for 8 h.

The obtained products of the initial synthesis were examined in terms of phase composition using the XRD method, with a particular focus on the formation of the ye'elimite phase (Table 3). In the case of set A, the desired phase was formed under all firing conditions, but its largest amounts (practically, the only product of synthesis) were found in the case of firing at 1350 °C/8 h. The synthesis of set C2 gave similar results. The synthesis

products of sets B and C contained ye'elimite, which, however, was also accompanied by other phases such as grossite, gehlenite, or hibonite. In the case of sample D, ye'elimite was identified in the products of synthesis, but the main phase was gehlenite. The synthesis products of samples E and F contained ye'elimite as one of the main phases, but—due to the presence of other chemical components in the starting materials—mineral phases were also identified, mainly larnite, i.e., dicalcium silicate Ca_2SiO_4, related to the presence of cement phase in the AC starting material. For most of the test samples, the increase in the firing temperature and the extension of the holding time from 4 to 8 h in the case of the highest assumed firing temperature resulted in the formation of the largest amount of the ye'elimite phase. An example comparison of the diffraction pattern in the range of the main reflex of ye'elimite—$Ca_4(AlO_2)_6SO_4$—is shown in Figure 7. For each variant, an increase in the reflex intensity and the appearance of a more "slender" reflex was observed, i.e., a decrease in the half-width with a simultaneous shift of the reflex maximum to lower angular values. This indicates an increase in the size of ye'elimite crystallites in the synthesized material.

Table 3. Determined amount of ye'elimite (XRD Rietveld method) in synthesized materials.

Conditions	Research Mix						
	A	**B**	**C**	**C2**	**D**	**E**	**F**
1250 °C/4 h	44.7 ± 1.0	46.1 ± 1.0	51.3 ± 1.1	87.6 ± 1.6	8.0 ± 0.6	54.7 ± 1.1	34.0 ± 0.9
1300 °C/4 h	50.2 ± 1.1	50.9 ± 1.0	61.3 ± 1.2	92.3 ± 1.6	15.9 ± 0.8	55.8 ± 1.2	37.3 ± 0.9
1350 °C/4 h	78.8 ± 1.4	54.7 ± 1.0	62.9 ± 1.2	98.0 ± 1.7	15.8 ± 0.8	60.2 ± 1.3	37.8 ± 1.1
1350 °C/8 h	98.8 ± 1.7	57.1 ± 1.1	61.1 ± 1.0	99.1 ± 1.7	15.5 ± 0.8	61.1 ± 1.3	38.5 ± 1.2

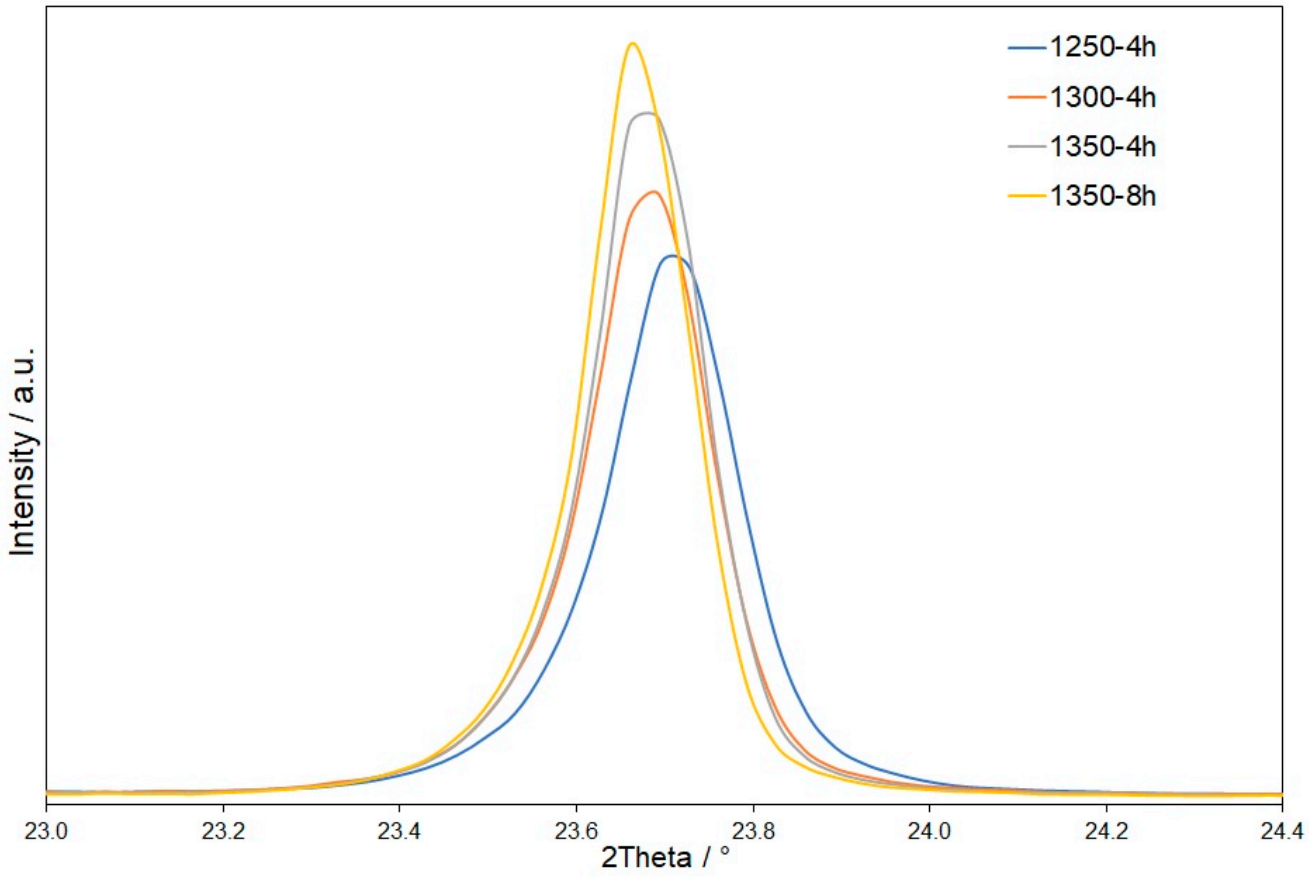

Figure 7. Changes of main ye'elimite XRD reflex for C2 series under different conditions of synthesis.

3.3. Proper Synthesis and Binder Properties

Based on the results obtained for the products of synthesis from the previous stage, 4 compositions (A, C2, E, and F) were selected for the proper synthesis. They were fired at 1350 °C and held for 8 h. This part of the research was aimed at preparing a sufficiently large amount of material to carry out tests related to the determination of the binding properties of the synthesis products. After the synthesis, phase composition was determined for each sample using XRD (Figure 8). Ye'elimite was identified as one of the main products in all of the synthesized materials, which was the aim of this study.

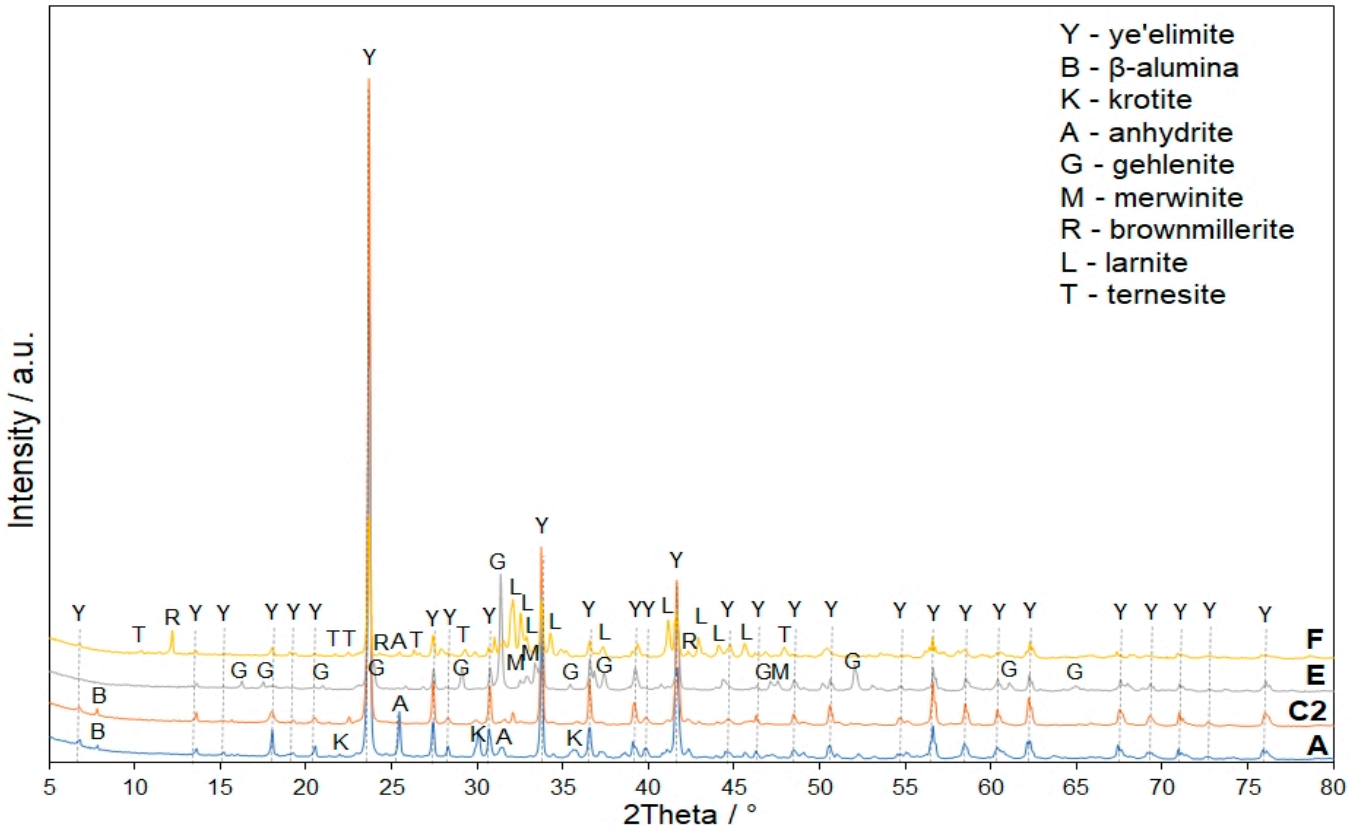

Figure 8. XRD patterns of the obtained materials after synthesis at 1350 °C/8 h.

In the case of material A, small amounts of anhydrite, crotite, and β-Al_2O_3 were also identified in the product. In material C2, only β-Al_2O_3 was present. The existence of these phases indicates an incomplete reaction of the raw materials with each other during the synthesis, which most probably resulted from the heterogeneous homogenization of the set composition. In areas that were rich in CaO and Al_2O_3 and, at the same time, devoid of sulfate ions, the synthesis proceeded toward the formation of crotite $CaAl_2O_4$. Moreover, the presence of slight amounts of sodium compounds in the raw material correcting the composition (Table 2, aluminum hydroxide) resulted in the incorporation of Na ions into the crystalline structure of aluminum oxide during the synthesis, producing the β-Al_2O_3 form.

In the case of materials based on AL and AC waste, the obtained X-ray diffraction patterns are more varied. Apart from the desired ye'elimite, gehlenite and mervinite (sample E) or larnite, brownmillerite, ternesite, and anhydrite (sample F) were also found. Their presence is directly related to the phase composition of the AL and AC materials used in the tests, especially the presence of silicon-containing compounds in the cement matrix of the AC waste.

Micrographs of the fractures of the materials obtained after synthesis are presented in Figure 9. The samples' microstructure can be described as a relatively homogeneous distribution of crystals, approximately 2–5-μm large. Observations at the same magnification,

however, reveal certain differences in the microstructure. The material obtained after the synthesis of mixture F is characterized by the largest grain, and the inter-grain boundaries are sharp and clearly visible. In the case of other materials, SEM images show clearly finer individual grains, but the grains of the synthesis product of A, C2, and E tend to form sintered, relatively compact conglomerates, with sample C2 exhibiting this property to the smallest degree.

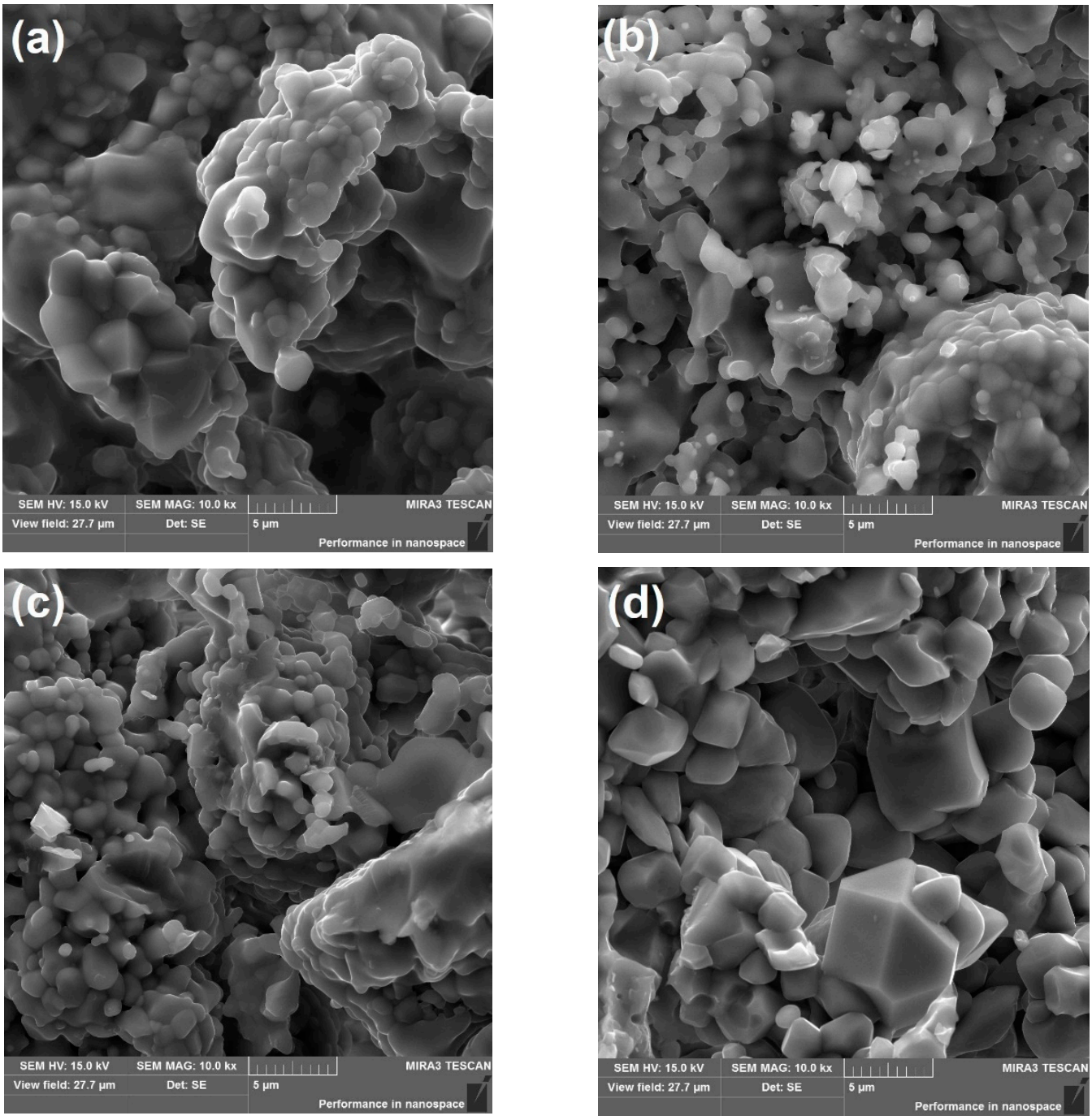

Figure 9. SEM images of the fracture of synthesized materials: A (**a**), C2 (**b**), E (**c**), and F (**d**).

The synthesized materials were also subjected to investigations into the initial characteristics of the obtained binders and binding properties by preparing appropriate mineral slurries based on the obtained products of synthesis (Table 4).

Table 4. Main properties of the obtained binders.

Feature	Research Mix			
	A	**C2**	**E**	**F**
water:binder ratio	0.30 ± 0.06	0.32 ± 0.06	0.29 ± 0.05	0.33 ± 0.06
bulk density; g/cm^3	3.0 ± 0.1	2.5 ± 0.1	3.2 ± 0.06	3.4 ± 0.07
specific surface; cm^2/g	6873 ± 1031	6319 ± 948	6278 ± 942	6220 ± 933
initial setting time; min	4 ± 1	13 ± 1	55 ± 2	50 ± 2
final setting time; h	0.2 ± 0.1	1.5 ± 0.1	5.3 ± 0.2	6.0 ± 0.2
flexular strength; MPa	4.0 ± 1.0	0.8 ± 0.2	1.6 ± 0.4	0.7 ± 0.2
compressive strength; MPa	37.5 ± 9.4	23.7 ± 5.9	13.4 ± 3.4	19.4 ± 4.9

All the materials had similar water requirements. The water–binder ratio oscillated around the value of 0.3, and more precisely, from 0.29 for material E to 0.33 for material E. Notably, the lowest value of bulk density is for material C2. This can be attributed to the relatively smallest grain and porosity visible in the fractures of the synthesized material during SEM observations (Figure 9b). The fragmentation of the material after synthesis resulted in obtaining powder materials with a significant surface development—for three samples, i.e., C2, E, and F, the specific surface area determined by the Blain method was at the level of approx. 6200–6300 cm^2/g. In the case of material A, a powder with a larger specific surface was obtained, which translated into better binding properties. For this sample, a very short setting time of approx. 12 min was obtained. However, it should be borne in mind that this material was synthesized only from reagents.

The binders obtained with the use of anthropogenic waste were characterized by significantly longer setting times. In the case of material C2, the end of setting was observed after approximately 90 min, while mixtures E and F set significantly longer, i.e., ca 5–6 h. Similarly, in the case of mechanical strength—compared to binder A, materials with an addition of anthropogenic waste displayed lower bending and compressive strength. In this case, however, it should be remembered that the product of synthesis (Table 3), apart from ye'elimite, also contained other mineral phases (Figure 8), which in a way, "dilute" the concentration of the main binding phase in the system.

4. Conclusions

In this preliminary study, the possibility of ye'elimite synthesis from anthropogenic waste sources has been presented. The following main conclusions can be formulated on the basis of the obtained results:

- The fibrous form of asbestos was destroyed in the thermal treatment process as a result of the crystal-chemical transformation;
- Asbestos waste, in combination with the aluminum anodizing material, was successfully transformed by high-temperature synthesis into a material containing ye'elimite as one of the main components;
- The obtained materials showed the ability to bind after mixing with water and had quite good physical and mechanical properties.

Due to the preliminary nature of the research undertaken in the project, it will be continued in order to optimize the composition and properties of the mineral binder with the use of waste, including asbestos–cement waste.

Author Contributions: Conceptualization, R.K.; methodology, R.K.; formal analysis, R.K., A.G., investigation, R.K., A.G., sources, B.L., R.K.; writing—original draft preparation, R.K., writing—review and editing, R.K., A.G. and B.L., visualization, R.K..; supervision, R.K., A.G. and B.L. All authors have read and agreed to the published version of the manuscript.

Funding: This research was funded in whole or in part by National Science Centre, Poland, under "Miniatura 5" grant number DEC-2021/05/X/ST5/00295. For the purpose of Open Access, the author has applied a CC-BY public copyright license to any Author Accepted Manuscript (AAM) version arising from this submission.

Data Availability Statement: Not applicable.

Conflicts of Interest: The authors declare no conflict of interest.

References

1. Gołaszewska, M.; Klemczak, B.; Gołaszewski, J. Thermal properties of calcium sulphoaluminate cement as an alternative to ordinary Portland cement. *Materials* **2021**, *14*, 7011. [CrossRef] [PubMed]
2. Harrison, T.; Roderick Jones, M.; Lawrence, D. The production of low energy cements. In *Lea's Chemistry of Cement and Concrete*, 5th ed.; Hewlett, P.C., Liska, M., Eds.; Butterworth-Heinemann: Oxford, UK, 2019; pp. 341–361. [CrossRef]
3. Chitvoranund, N.; Lothenbach, B.; Winnefeld, F.; Skibsted, J.; Scrivener, K. Comparison of different preparation methods for ye'elimite clinker synthesis. In Proceedings of the International Workshop on Calcium Sulfoaluminate Cements, Murten, Switzerland, 4–6 June 2018; p. 22.
4. Julphunthong, P.; Joyklad, P. Utilization of several industrial wastes as raw material for calcium sulfoaluminate cement. *Materials* **2019**, *12*, 3319. [CrossRef] [PubMed]
5. Batog, M.; Synowiec, K.; Dziuk, D. Cement i spoiwa specjalne zawierające klinkier siarczanoglinianowy. *BTA* **2017**, *2*, 59–64. (In Polish)
6. Ioannou, S.; Reig, L.; Paine, K.; Quillin, K. Properties of a ternary calcium sulfoaluminate-calcium sulfate-fly ash cement. *Cem. Concr. Res.* **2014**, *56*, 75–83. [CrossRef]
7. Di Maio, F.; Rem, P.C. A robust indicator for promoting circular economy through recycling. *J. Environ. Prot.* **2015**, *6*, 1095–1104. [CrossRef]
8. Corona, B.; Shen, L.; Reike, D.; Carreón, J.R.; Worrell, E. Towards sustainable development through the circular economy—A review and critical assessment on current circularity metrics. *Resour. Conserv. Recycl.* **2019**, *151*, 104498. [CrossRef]
9. Ministry of Environment of the Republic of Poland. Regulation of the Minister of the Environment of 27 September 2001 on the waste catalog (Journal of Laws No. 112, item 1206). (In Polish). Available online: https://isap.sejm.gov.pl/isap.nsf/DocDetails.xsp?id=wdu20011121206 (accessed on 10 October 2022).
10. Sejm of the Republic of Poland. Waste Act of 14 December 2012 with later changes (Journal of Laws 2013, item 21). (In Polish). Available online: https://isap.sejm.gov.pl/isap.nsf/DocDetails.xsp?id=WDU20130000021 (accessed on 10 October 2022).
11. Dijkstra, J.J.; Comans, R.N.J.; Schokker, J.; van der Meulen, M.J. The geological significance of novel anthropogenic materials: Deposits of industrial waste and by-products. *Anthropocene* **2019**, *28*, 100229. [CrossRef]
12. European Parliament resolution of 14 March 2013 on asbestos related occupational health threats and prospects for abolishing all existing asbestos (2012/2065(INI)). Available online: https://eur-lex.europa.eu/legal-content/EN/TXT/?uri=CELEX%3A52013IP0093 (accessed on 10 October 2022).
13. Council of Ministers of the Republic of Poland. *Program for the Removal of Asbestos and Asbestos-Containing Products Used in Poland*; Polish Government: Warsaw, Poland, 2002. (In Polish)
14. Obmiński, A. *Asbestos in Buildings*; Building Research Institute: Warsaw, Poland, 2017. (In Polish)
15. Wallis, S.L.; Emmett, E.A.; Hardy, R.; Casper, B.B.; Blanchon, D.J.; Testa, J.R.; Menges, C.W.; Gonneau, C.; Jerolmack, D.J.; Seiphoori, A.; et al. Challenging global waste management—Bioremediation to detoxify asbestos. *Front. Environ. Sci.* **2020**, *8*, 20. [CrossRef]
16. Li, J.; Dong, Q.; Yu, K.; Liu, L. Asbestos and asbestos waste management in the Asian-Pacific region: Trends, challenges and solutions. *J. Clean. Prod.* **2014**, *81*, 218–226. [CrossRef]
17. Frank, A.L.; Joshi, T.K. The global spread of asbestos. *Ann. Glob. Health.* **2014**, *80*, 257–262. [CrossRef]
18. International Ban Asbestos Secretariat. Available online: http://www.ibasecretariat.org/ (accessed on 10 October 2022).
19. Flanagan, D.M. *Mineral Commodity Summaries. Asbestos 2021*; U.S. Geological Survey: Reston, VA, USA, 2022.
20. Gualtieri, A.F. Recycling asbestos-containing material (ACM) from construction and demolition waste (CDW). In *Handbook of Recycled Concrete and Demolition Waste*; Pacheco-Torgal, F., Tam, V.W.Y., Labrincha, J.A., Ding, Y., de Brito, J., Eds.; Woodhead Publishing: Cambridge, UK, 2013; Volume 47, pp. 500–525. [CrossRef]
21. Spasiano, D.; Pirozzi, F. Treatments of asbestos containing wastes. *J. Environ. Manag.* **2017**, *204*, 82–91. [CrossRef] [PubMed]
22. Paolini, V.; Tomassetti, L.; Segreto, M.; Borin, D.; Liotta, F.; Torre, M.; Petracchini, F. Asbestos treatment technologies. *J. Mater. Cycles Waste Manag.* **2019**, *21*, 205–226. [CrossRef]
23. Brown, S.K. Asbestos exposure during renovation and demolition of asbestos-cement clad buildings. *Am. Ind. Hyg. Assoc. J.* **1987**, *28*, 478–486. [CrossRef] [PubMed]
24. Obmiński, A.; Janeczek, J. The effectiveness of asbestos stabilizers during abrasion of asbestos-cement sheets. *Constr. Build. Mater.* **2020**, *249*, 118767. [CrossRef]
25. Ribeiro, M.J.; Tulyaganov, D.U.; Ferreira, J.M.; Labrincha, J.A. Recycling of Al-rich industrial sludge in refractory ceramic pressed bodies. *Ceram. Int.* **2002**, *28*, 319–326. [CrossRef]

26. Pereira, D.A.; Couto, D.M.; Labrincha, J.A. Incorporation of aluminum-rich residues in refractory bricks. *CFI—Ceram. Forum Int.* **2000**, *77*, 21–25.
27. Gualtieri, A.F.; Cavenati, C.; Zanatto, I.; Meloni, M.; Elmi, G.; Gualtieri, M.L. The transformation sequence of cement–asbestos slates up to 1200 °C and safe recycling of the reaction product in stoneware tile mixtures. *J. Hazard. Mater.* **2008**, *152*, 563–570. [CrossRef]
28. Kusiorowski, R.; Zaremba, T.; Piotrowski, J.; Podwórny, J. Utilisation of cement-asbestos wastes by thermal treatment and the potential possibility use of obtained product for the clinker bricks manufacture. *J. Mater. Sci.* **2015**, *50*, 6757–6767. [CrossRef]
29. Kusiorowski, R.; Zaremba, T.; Piotrowski, J.; Adamek, J. Thermal decomposition of different types of asbestos. *J. Therm. Anal. Calorim.* **2012**, *109*, 693–704. [CrossRef]
30. Vergani, F.; Galimberti, L.; Marian, N.M.; Giorgetti, G.; Viti, C.; Capitani, G.C. Thermal decomposition of cement-asbestos at 1100 °C: How much "safe" is "safe"? *J. Mater. Cycles Waste Manag.* **2022**, *24*, 297–310. [CrossRef]
31. *PN-EN ISO 12677:2011*; Standard. Chemical Analysis of Refractory Products by X-ray Fluorescence (XRF)—Fused Cast-Bead Method. ISO: Geneva, Switzerland, 2011.
32. Viani, A.; Gualtieri, A.F.; Secco, M.; Peruzzo, L.; Artioli, G.; Cruciani, G. Crystal chemistry of cement-asbestos. *Am. Mineral.* **2013**, *98*, 1095–1105. [CrossRef]
33. Kusiorowski, R.; Zaremba, T.; Piotrowski, J.; Gerle, A. Thermal decomposition of asbestos-containing materials. *J. Therm. Anal. Calorim.* **2013**, *113*, 179–188. [CrossRef]
34. Viani, A.; Gualtieri, A.F.; Pollastri, S.; Rinaudo, C.; Croce, A.; Urso, G. Crystal chemistry of the high temperature product of transformation of cement-asbestos. *J. Hazard. Mater.* **2013**, *248*, 69–80. [CrossRef] [PubMed]
35. Viani, A.; Gualtieri, A.F. Recycling the product of thermal transformation of cement-asbestos for the preparation of calcium sulfoaluminate clinker. *J. Hazard. Mater.* **2013**, *260*, 813–818. [CrossRef] [PubMed]
36. Gualtieri, A.F. *Mineral Fibers: Crystal Chemistry, Chemical-Physical Properties, Biological Interaction and Toxicity*; European Mineralogical Union: London, UK, 2017; Volume 18.